Salt transport in the near-surface layer in the monsoon-influenced Indian Ocean using HYCOM

Ebenezer S. Nyadjro,[1] Bulusu Subrahmanyam,[1,2] V. S. N. Murty,[3] and Jay F. Shriver[4]

Received 27 May 2010; accepted 29 June 2010; published 4 August 2010.

[1] Salt advection in the top 5 m layer of the monsoon-influenced Indian Ocean has been studied with high resolution HYbrid Coordinate Ocean Model (HYCOM) simulated sea surface salinity (SSS) during 2003-06. The effect of monsoon reversals and roles of Ekman drift and geostrophic currents are emphasized. The Ekman drift component is found to be more important than the geostrophic component in exchange of salt in the basins; an indication of the influence of winds and the associated surface currents. The strongest differences in the salt advection terms occurred in the Bay of Bengal (BoB), an indication of the significant role of advection for the distribution of freshwater and the Ekman processes. The Inter-Tropical Convergence Zone (ITCZ) is seen to influence advection patterns via Ekman drift along the equatorial region. This results in the creation of two salt advection bands whose positions vary seasonally. This study will help to interpret data from the recently launched Soil Moisture Ocean Salinity (SMOS) and future Aquarius salinity missions for the Indian Ocean. **Citation:** Nyadjro, E. S., B. Subrahmanyam, V. S. N. Murty, and J. F. Shriver (2010), Salt transport in the near-surface layer in the monsoon-influenced Indian Ocean using HYCOM, *Geophys. Res. Lett.*, *37*, L15603, doi:10.1029/2010GL044127.

1. Introduction

[2] The Indian Ocean shows significant variability in the distribution of sea surface salinity (SSS), especially in the two northern basins, the Bay of Bengal (BoB) and the Arabian Sea (AS) [*Murty et al.*, 2004; *Joseph and Freeland*, 2005]. The seasonal reversal of monsoon winds and the differences in precipitation (P), evaporation (E) and river runoff (R) makes the BoB a net precipitation basin and the AS a net evaporative basin [*Sengupta et al.*, 2006]. Also the northern Indian Ocean shows larger SSS variability than the southern Indian Ocean [*Rao and Sivakumar*, 2003]. In order to balance salt and mass, there is the need for exchange between the basins. The dynamics of ocean salt distribution have been studied in some works. *Delcroix and Henin* [1991] analyzed and discussed equations for SSS changes in the tropical Pacific Ocean. They concluded that the meridional Ekman salt transport played a more significant role in salinity distribution than zonal salt transport. Additionally it was important for the displacement of low saline water from regions where E exceeded P such as the ITCZ and the South Pacific Convergence Zone (SPCZ).

[3] Basin-wide scale studies of SSS dynamics in the Indian Ocean have been a challenge and limiting as a result of paucity of observations of SSS. Thus, the mechanisms for the transport of salt in the Indian Ocean are not fully understood. Global HYCOM simulated SSS data, validated with *in situ* observations by *Heffner et al.* [2008], is used in order to make a basin-scale study of SSS dynamics in the Indian Ocean.

[4] *Delcroix and Henin* [1991] expressed the time-averaged salt conservation equation for the mixed layer as:

$$\frac{\partial S}{\partial t} = -U\frac{\partial S}{\partial x} - V\frac{\partial S}{\partial y} + h^{-1}\frac{dh}{dt}H\left(\frac{dh}{dt}\right).(S - S_{z=h}) + h^{-1}(E-P)S \quad (1)$$

where S is salinity, U the zonal component of velocity, V the meridional component of velocity, h the depth of the upper mixed layer (here only the surface HYCOM layer, which corresponds to the depth range 0–5 m, is used), $S_{z=h}$ the salinity just below the mixed layer depth, H the Heaviside step function, E the evaporation, and P the precipitation. In the HYCOM SSS, the E-P and river run off components are included. Vertical advection is usually not considered as the mixed layer salinity is assumed to be uniform as that of SSS. For this reason, equation (1) could be considered valid for SSS [*Delcroix and Henin*, 1991]. In furtherance of this, we examine particularly, the first two terms of equation (1) and their effects on SSS transport. Because of the significant effect of Ekman forcing by monsoonal winds and its generation of monsoonal currents in the Indian Ocean [*Snankar et al.*, 1996; *Murtugudde et al.*, 2007], we split the horizontal advection into Ekman drift and geostrophic current components in order to understand their relative roles, magnitudes and effects in the transport of SSS in the Indian Ocean. We believe that the basin-wide details of such studies are presently inexplicit in literature.

[5] This paper hopes to contribute towards understanding the dynamics of salt distribution in the Indian Ocean. The strong annual variability in winds and water circulation, and its impact on the distribution of SSS also makes the Indian Ocean a good laboratory for the calibration and validation of the anticipated satellite-derived SSS from the recently launched European Space Agency's (ESA) Soil Moisture and Ocean Salinity (SMOS) and NASA and Space Agency of Argentina's (Comision Nacional de Actividades Espaciales, CONAE) Aquarius/SAC-D satellite missions. The 1/12° high horizontal resolution of the HYCOM model and its smooth transition to a terrain-following coordinate in coastal

[1]Marine Science Program, University of South Carolina, Columbia, South Carolina, USA.
[2]Department of Earth and Ocean Sciences, University of South Carolina, Columbia, South Carolina, USA.
[3]National Institute of Oceanography Regional Center, Visakhapatnam, India.
[4]Naval Research Laboratory, Stennis Space Center, Mississippi, USA.

0094-8276/10/2010GL044127

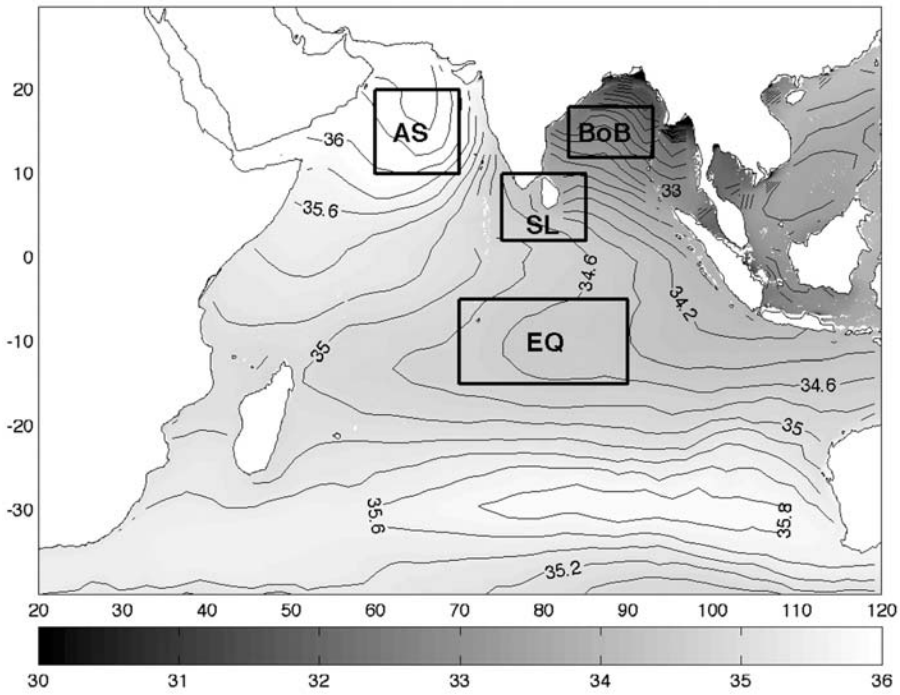

Figure 1. Four-year mean HYCOM salinity with boxes denoting the averaging sub-regions for the study; Arabian Sea (AS), Bay of Bengal (BoB), Sri Lanka (SL), and Equatorial (EQ) regions.

regions will especially help in the retrieval, calibration and validation of satellite data in coastal areas where sensor L-band measurements are affected by nearby lands and significant variability in river plumes. Further, the river run off from the major and minor rivers of the Indian Ocean, particularly into the Bay of Bengal, is included in the HYCOM SSS simulations.

2. Data and Methods

[6] This study uses the 4 year period (2003–2006) monthly SSS from the global HYbrid Coordinate Ocean Model (HYCOM) with 1/12° horizontal resolution, a description of which is provided and validated with *in situ* observations by *Heffner et al.* [2008]. The height of the sea surface above a level surface ζ, was obtained from TOPEX/Poseidon, and Jason-1 altimetry. The surface wind stress $\tau = \rho_a C_D \psi$ was computed from the Florida State University's (FSU) Center for Ocean-Atmosphere Prediction Studies (COAPS) 1° × 1° gridded pseudo-stress (ψ) data with ρ_a = 1.2041 kg/m^3 and C_D = 0.0015 [*Bourassa et al.*, 2005]. Geostrophic component of the horizontal salt transport was estimated from

$$U_{gs} = -U_g \frac{\partial S}{\partial x} \text{ and } V_{gs} = -V_g \frac{\partial S}{\partial y} \quad (2)$$

where S is salinity, U_g and V_g are surface geostrophic currents computed respectively from

$$U_g = -\frac{g}{f}\frac{\partial \zeta}{\partial y} \text{ and } V_g = \frac{g}{f}\frac{\partial \zeta}{\partial x} \quad (3)$$

where g is acceleration due to gravity (9.8 ms^{-2}), f is the Coriolis parameter ($2\Omega \sin\phi$).

[7] Ekman wind drift component of the horizontal salt transport was estimated from

$$U_{es} = -U_e \frac{\partial S}{\partial x} \text{ and } V_{es} = -V_e \frac{\partial S}{\partial y} \quad (4)$$

where U_e and V_e are the surface Ekman drift computed respectively from $U_e = \frac{\tau_y}{\rho_o f h}$ and

$$V_e = \frac{-\tau_x}{\rho_o f h} \quad (5)$$

whereas 'h' is 5 m depth, selected as the depth of stability maximum in the salinity stratified layer, ρ_o is the water density (1023 kg m^{-3}). Finally, surface salinity transport is computed from

$$F_s = vH\Delta S \quad (6)$$

Where F_s is the salt transport in psu m^{2}s^{-1}, v is the magnitude of HYCOM current velocity in ms^{-1}, H is the first model layer depth in the HYCOM model (~5 m) and ΔS is the salinity anomaly in psu. ΔS is determined from $\Delta S = S - \overline{S}$, where $\overline{S}$ is the annual mean SSS.

3. Results and Discussion

[8] Four-year mean HYCOM SSS (Figure 1) shows four main regions of salinity distribution. The highest and lowest values are recorded in the AS and BoB respectively. The region south of 5°S have values between those of the AS and BoB. The seasonal difference in the AS and BoB is well simulated by the HYCOM and consistent with observational data [*Rao and Sivakumar*, 2003]. The differences between the two basins can be attributed to freshwater forcing

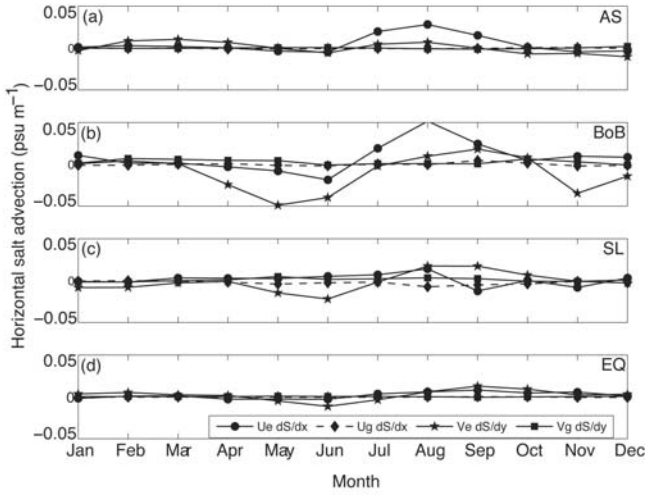

Figure 2. Four-year mean variation of horizontal salt advection terms in (a) AS, (b) BoB, (c) SL, and (d) EQ.

especially during the SW monsoon (June–September) when precipitation exceeds evaporation in the BoB and vice versa in the AS. The low salinity tongue along the 10°S latitude is a consequence of the Indonesian Throughflow (ITF) and the flow of BoB low salinity waters [*Sengupta et al.*, 2006].

[9] The contributions from the salinity advection terms (U_{es}, U_{gs}, V_{es} *and* V_{gs}) in the different sub-regions show seasonal and spatial variations (Figures 2a–2d). The strongest differences in the Ekman component are seen in the BoB, where the minimum occurred in May and November (southward Ekman component), and the maximum occurred in August (eastward Ekman component), emphasizing the influence of freshwater in salt transport especially during the months of monsoon-transition and SW monsoon.

[10] The Ekman components of salt transport are more significant and 4 times higher than the geostrophic components (Figure 3). Summarily, the meridional salt advection has a greater influence on SSS transport than zonal salt advection (Figure 3). During the NE monsoon season (November–February), there is not much difference in the four components of the SSS advection in the four regions (Figures 1 and 2) except during November – December when salinity transport was dominated by the southward Ekman component in the BoB (Figure 2b). This transports low saline waters from the BoB, leading to increased SSS along western BoB. During this season, winds are predominantly from the NE, and the Ekman drift is westward and stronger in the western BoB [*Snankar et al.*, 1996], reflecting in the advection patterns during this time. Although the dry NE winds result in higher evaporation (another reason for high SSS in western BoB), the eastern BoB water is still low in SSS during winter following the influx of summer's river runoff. In January and February, salinity advection in the BoB slows down, with the geostrophic components being more important, an indication of weakened wind effect. NE monsoon salinity advection is lower in the AS compared to the BoB, with the significant advections being southward along the Somali current region and dominated by Ekman drift. The rest of the AS region shows patchy geostrophic contributions, possibly an influence of intermittent eddies. These eddy-influenced transports also occur in the southeastern Indian Ocean where the winter advection is predominately westward geostrophic flow. Although *Han and McCreary* [2001] observed Ekman drift in this region to increase at the peak of the NE monsoon, local Ekman pumping forces the geostrophic flow. NE monsoon SSS advection around the Sri Lankan region indicates the contributions and influence of different mechanisms. At the start of the NE monsoon season, the Ekman component reduces in magnitude and reverses from eastward to westward, transporting water into the AS. The geostrophic component becomes southward and lesser in magnitude than the Ekman component. At the peak of the NE monsoon, all the components are about the same magnitude except the Ekman component which becomes very significant (Figure 2). Geostrophic contribution to SSS advection around the equatorial region was low compared to the Ekman component which shows two distinct continuous bands, with the SW monsoon advection being stronger than the NE monsoon (Figures 3e–3h). During winter, there is a band of positive salt advection on either side of the equator, with the upper band having a northward flow whiles the lower band has a southward flow. During the summer, both bands lie on the southern side of the equator with the upper band flowing northward while the lower band flows southward, a reverse of the winter's pattern. The pattern could be linked to the dynamics of the ITCZ. During the NE monsoon, the ITCZ migrates southward, and strengthens the NE trade winds that enhance evaporation. The westward extent of these bands could also be attributed to the pathway and influence of the ITF.

[11] The seasonal cycle of salinity transport estimated in the upper 5 m layer from equation (6) using the magnitude of current velocity and the SSS anomaly (monthly HYCOM SSS – annual mean HYCOM SSS) in each grid point is presented in Figure 4. We present the bi-monthly maps of salinity transport from October (Figures 4a–4f). This SSS transport considers the model SSS (the E-P and river run off components are included) and the model current velocity and hence represents the total magnitude of salinity transport, without bifurcating into geostrophic and Ekman components of SSS transport.

[12] In October, a band of fresh water advection (negative salinity transport) is noticed along the east coast of India and the eastern rim of the Bay and northern Sumatra coast (Figure 4a). This low salinity water transport along the east coast of India is due to the southward flowing East India Coastal Current (EICC) along the coast soon after the withdrawal of the southwest monsoon winds. *McCreary et al.* [1993] and *Snankar et al.* [1996] reported that the southward EICC is remotely driven by the downwelling Kelvin Waves. Interestingly, during October, the southeastern Arabian Sea and south of Sri Lanka are the regions of high salinity (positive salinity transport). The South Equatorial Current (SEC) in the southern tropical Indian Ocean transports anomalously high salinity waters towards west along 12–16°S. The ITF originating from the Pacific Ocean flows into the SEC. *Potemra* [2005] mentions that the ITF transport is maximum in general during July–October, the period of SW monsoon and is weak during NE monsoon. Low salinity waters of the Pacific origin are advected into the Indian Ocean through the ITF. This observed anomalous high salinity waters may be due to the weakening of the ITF during the observational period (2003-06) under the influ-

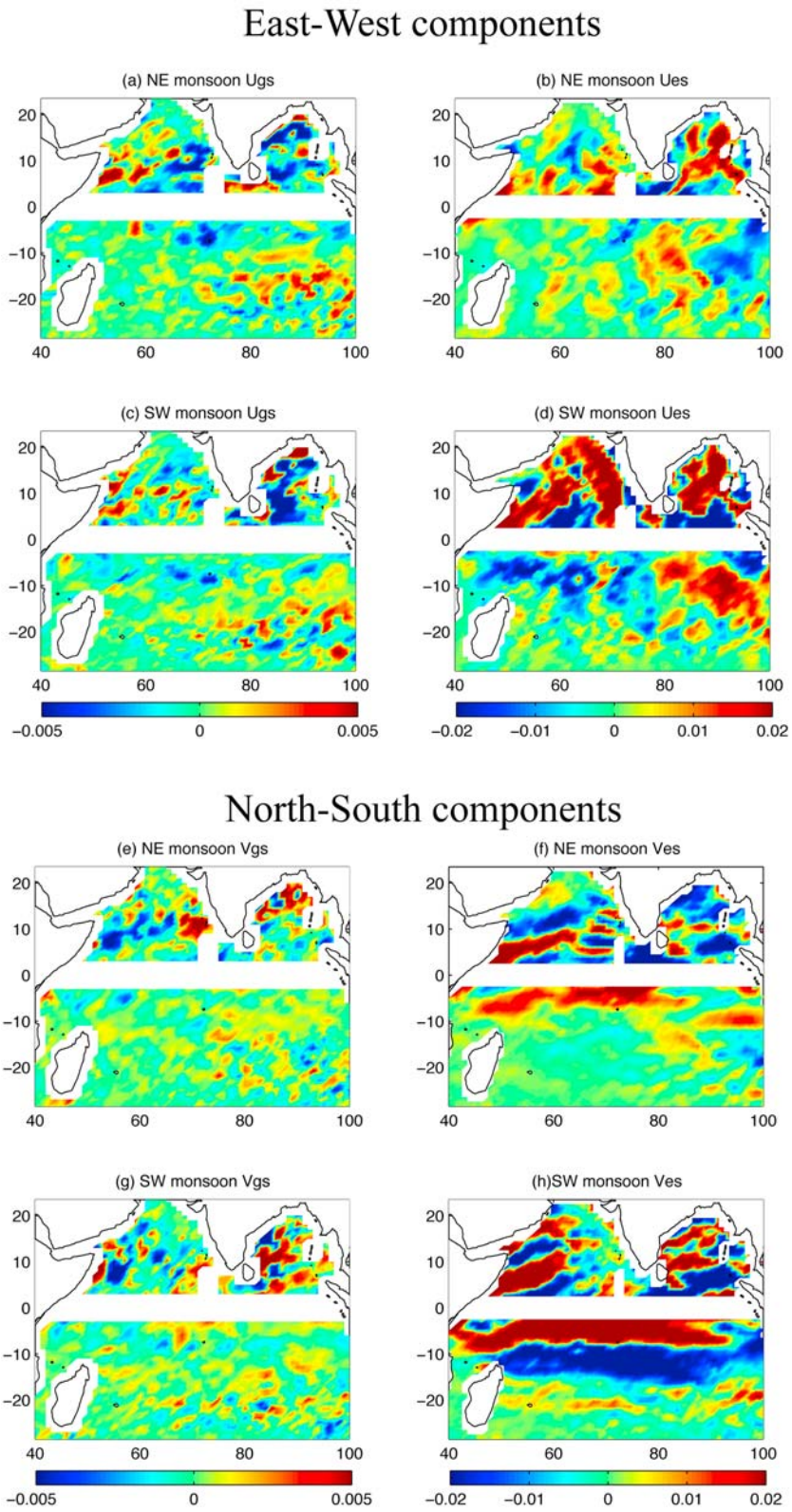

Figure 3. Four-year mean (top) East–West components and (bottom) North–South components of geostrophic and Ekman drift of salinity advection during the (a, b, e, and f) Northeast and (c, d, g, and h) Southwest monsoon seasons; Geostrophic and Ekman drifts are computed with the negative sign as described in equations (2) and (4). Units are psu ms^{-1}.

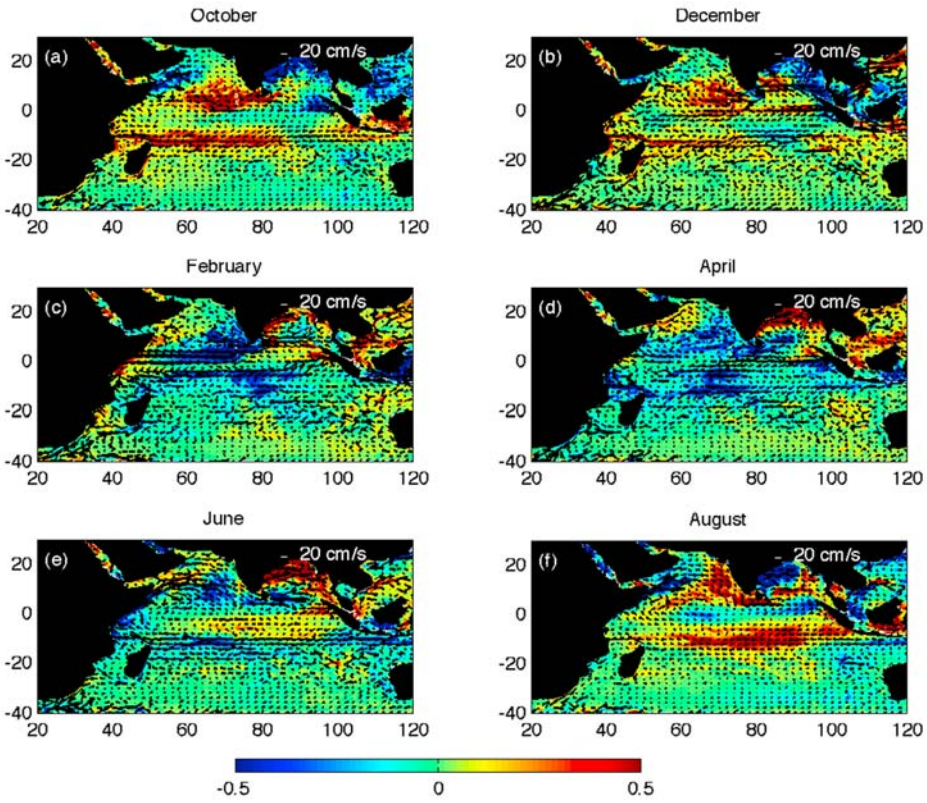

Figure 4. Bi-monthly maps of salinity transport (m^2s^{-1}) with overlaid surface velocity vectors ($m.s^{-1}$) during (a) October, (b) December, (c) February, (d) April, (e) June and (f) August.

ence of the Indian Ocean Dipole events [*Vinayachandran et al.*, 2007]. Off northern Sumatra, a pocket of low salinity water transport is noticed while along the southern Sumatra a pocket of high salinity transport is seen. By December, the eastern Bay transports low SSS waters towards Sumatra coast and then westwards into the SEC. This observation is in agreement with that of *Jensen* [2001] and *Sengupta et al.* [2006] (Figure 4b).

[13] By February, the western Bay and the east coast of India transports high salinity waters poleward and the North Equatorial Counter Current (NECC) in the Southern Bay also transports high SSS waters (Figure 4c). The Southeastern Arabian Sea and Southern Arabian Sea are now replaced with the lower SSS and extends into the southwestern Arabian Sea. A band of low salinity water transport is located at 10°S. It is interesting to note that both the western Arabian Sea and western Bay of Bengal transport high salinity waters. However, the higher SSS in the western Bay of Bengal is transported poleward and the high SSS waters in the western Arabian Sea are transported equatorward by the reversing Somali current during NE monsoon (Figure 4c). The open ocean regions (southeastern Arabian Sea and south of equator) are characterized with the low SSS transport. Part of the low SSS transport in the southeastern Arabian Sea is due to the transport of the southward EICC in December and its further extension into the Southeastern Arabian Sea by February.

[14] By April, the low SSS ITF is seen as a band along 10°S and its extension into the Somali region along the East African Coast is evident, thus giving the evidence to the contribution of ITF into the salt budget of the Arabian Sea (Figure 4d). While the high SSS transport extends into the central Arabian Sea from the Oman coast, the low SSS waters of NE monsoon in the Southeastern Arabian Sea weakened. High SSS transport in the western Bay is strengthened by the strength of the poleward EICC (Figure 4d). By May, a band of high SSS transport associated with the eastward flowing Spring Wyrtki Jet is noticed in the eastern equatorial region (figure not shown). The Ekman transport of the spring intermonsoon winds brings in back the low SSS waters from the Southeastern Arabian Sea, into the Sri Lanka region. Compared to the SSS transport in October (Figure 4a), the SSS transport off Sumatra is opposite in May (figure not shown). With the advancement of the southwest monsoon, the SSS transport showed large variation (Figures 4e and 4f).

[15] By July/August, the Southeastern Arabian Sea occupies with high SSS waters, and Somali current transports low SSS waters into the Arabian Sea. These low SSS waters in the Somali Currents are of the ITF origin during April–June (Figures 4d and 4e). The western Bay of Bengal once again becomes the source of low salinity waters from monsoon precipitation and river runoff. The ITF anomalously becomes weak during July–August during the observation period (2003-06), as can be seen from the band of high SSS transport along 10°S. Advection of high SSS waters into the Bay of Bengal during August–September is evident during Southwest monsoon (Figure 4f).

4. Conclusions

[16] The seasonal variability of SSS in the Indian Ocean as seen in observational data is well simulated by HYCOM;

SSS in the Arabian Sea is in general higher than that in the Bay of Bengal. Analysis of the contributions of Ekman drift and geostrophic current shows the former's dominance in the SSS distribution in the Indian Ocean indicating the influence of wind in the transport process. Although these vary both spatially and temporally, on the whole meridional transport dominated over zonal transport. The transport of low saline waters into the Arabian Sea during the SW monsoon is seen to originate from the ITF during April–June. High saline Arabian Sea water is transported into the Bay of Bengal along the Sri Lankan coast by strong geostrophic and Ekman contributions. We noticed the anomalously weak ITF during the observation period (2003-06) under the influence of Indian Ocean Dipole.

[17] **Acknowledgments.** This work was supported in part by the NASA project NNX08AO33G awarded to BS. JS was supported by the 6.1 project "Global and Remote Littoral Forcing in Global Ocean Models" sponsored by the Office of Naval Research (ONR) under program element 601153N. The authors would like to thank two anonymous reviewers for all their helpful comments and suggestions. This has the NIO contribution number 4794.

References

Bourassa, M. A., R. Romero, S. Smith, and J. O'Brien (2005), A new FSU winds climatology, *J. Clim.*, *18*, 3686–3698, doi:10.1175/JCLI3487.1.

Delcroix, T., and C. Henin (1991), Seasonal and Interannual variations of the sea surface salinity in the tropical Pacific Ocean, *J. Geophys. Res.*, *96*, 22,135–22,150, doi:10.1029/91JC02124.

Han, W., and J. P. McCreary (2001), Modeling salinity distributions in the Indian Ocean, *J. Geophys. Res.*, *106*, 859–877, doi:10.1029/2000JC000316.

Heffner, D. M., B. Subrahmanyam, and J. F. Shriver (2008), Indian Ocean Rossby waves detected in HYCOM sea surface salinity, *Geophys. Res. Lett.*, *35*, L03605, doi:10.1029/2007GL032760.

Jensen, T. G. (2001), Arabian Sea and Bay of Bengal exchange of salt and tracers in an ocean model, *Geophys. Res. Lett.*, *28*, 3967–3970, doi:10.1029/2001GL013422.

Joseph, S., and H. J. Freeland (2005), Salinity variability in the Arabian Sea, *Geophys. Res. Lett.*, *32*, L09607, doi:10.1029/2005GL022972.

McCreary, J. P., P. K. Kundu, and R. L. Molinari (1993), A numerical investigation of the dynamics, thermodynamics and mixed-layer processes in the Indian Ocean, *Prog. Oceanogr.*, *31*, 181–244, doi:10.1016/0079-6611(93)90002-U.

Murtugudde, R., R. Seager, and P. Thoppil (2007), Arabian Sea response to monsoon variations, *Paleoceanography*, *22*, PA4217, doi:10.1029/2007PA001467.

Murty, V. S. N., B. Subrahmanyam, V. Tilvi, and J. J. O'Brien (2004), A new technique for the estimation of sea surface salinity in the tropical Indian Ocean from OLR, *J. Geophys. Res.*, *109*, C12006, doi:10.1029/2003JC001928.

Potemra, J. T. (2005), Indonesian Throughflow transport variability estimated from satellite altimetry, *Oceanography*, *18*(4), 98–107.

Rao, R. R., and R. Sivakumar (2003), Seasonal variability of sea surface salinity and salt budget of the mixed layer of the north Indian Ocean, *J. Geophys. Res.*, *108*(C1), 3009, doi:10.1029/2001JC000907.

Sengupta, D., G. N. Bharath Raj, and S. S. C. Shenoi (2006), Surface freshwater from Bay of Bengal runoff and Indonesian Throughflow in the tropical Indian Ocean, *Geophys. Res. Lett.*, *33*, L22609, doi:10.1029/2006GL027573.

Snankar, D., J. P. McCreary, W. Han, and S. R. Shetye (1996), Dynamics of the East Indian Coastal Current: 1. Analytic solutions forced by interior Ekman pumping and local alongshore winds, *J. Geophys. Res.*, *101*, 13,975–13,991, doi:10.1029/96JC00559.

Vinayachandran, P. N., J. Kurin, and C. P. Neema (2007), Indian Ocean response to anomalous conditions during 2006, *Geophys. Res. Lett.*, *34*, L15602, doi:10.1029/2007GL030194.

V. S. N. Murty, National Institute of Oceanography Regional Centre, 176, Lawsons Bay Colony, Visakhapatnam 530 017, India.

E. S. Nyadjro and B. Subrahmanyam, Marine Science Program, University of South Carolina, EWS 603, 712 Main St., Columbia, SC 29208, USA. (sbulusu@geol.sc.edu)

J. F. Shriver, Naval Research Laboratory, Code 7323, Bldg. 1009, Stennis Space Center, MS 39529, USA.